Available online at https://asric.africa/natural-sciences
ASRIC Journal on Natural Sciences Vol 4(1) (2024) 39-48

Damage-Sensing Capabilities of GFRP Composites through Carbon Nanofillers for Advanced Structural Health Monitoring

Eman. O. Taha[1*], Usama F. Kandil[1], G. M. Nasr[2], and Mahmoud Reda Taha[3]

[1]Petroleum Applications Department, Egyptian Petroleum Research Institute, Cairo, Egypt.
[2]Physics Department, Faculty of Science, Cairo University, Giza, Egypt.
[3]Department of Civil Engineering, University of New Mexico, Albuquerque, NM 87131, USA.

* Correspondence author: eman.omar2006@gmail.com, eman.omar@epri.sci.eg

Received 11 March 2024; revised 26 April 2024; accepted 30 May 2024

Abstract

This study investigates the use of carbon nanofillers, specifically multi-walled carbon nanotubes (MWCNTs) and carbon nanofibers (CNFs), to enhance the damage-sensing capabilities of glass fiber-reinforced epoxy (GFRP) composites. Nanocomposites were fabricated by incorporating 2.0 wt.% of MWCNTs and CNFs into the epoxy matrix, followed by mechanical and electrical testing. The results demonstrated significant improvements, with the fatigue life increasing by 165% for CNFs/GFRP and 218% for MWCNTs/GFRP compared to neat GFRP. Stiffness also increased due to the re-orientation of nanofillers during cyclic loading. Electrical conductivity changes, measured in real time, provided a reliable metric for detecting damage, particularly microcracks. CNFs/GFRP composites showed superior sensitivity, with up to 100% conductivity change, making them ideal for real-time structural health monitoring. These findings highlight the potential for using carbon nanofillers in advanced smart composites, with applications in industries such as aerospace and civil engineering. Future research should explore optimizing nanofiller performance and investigating other composite materials for enhanced damage detection and durability.

Keywords: Damage Sensing, GFRP, Carbon Nanotubes, Carbon Nanofibers, Fatigue Loading, Engineering applications.

Introduction

Structural health monitoring (SHM) aims to diagnose material conditions during operation, offering a significant improvement over traditional inspection methods(Wang et al., 2014). It enhances safety and operational efficiency across industries by detecting structural deterioration early, preventing failures, financial losses, and casualties. SHM also provides design engineers with valuable data to improve system performance and material choices. Various sensors, such as strain gauges(Anas et al., 2018), acoustic emission sensors(Finlayson et al., 2001), fiber Bragg gratings(Li et al., 2006), and smart sensors, can be integrated into SHM systems. However, the challenge lies in embedding these sensors without affecting the structure's weight or performance. Ideally, sensors are integrated during manufacturing to avoid additional costs.

Composite materials present a solution due to their customizable properties, including self-sensing capabilities. These "smart composites" can be tailored through the selection of fibers, fillers, and matrix materials and are a key area of research(Dong et al., 2016; Güemes et al., 2020). Fiber-reinforced polymers (FRPs), widely used in aerospace, wind energy industries, transport, and defense, are valued for their high strength-to-weight ratios(GangaRao, 2017; Liang & GangaRao, 2004). However, their non-homogeneous nature leads to unique failure mechanisms. While conventional SHM methods apply to FRPs, embedded sensors offer the advantage of real-time damage monitoring without removing the structure from service. In carbon fiber-reinforced plastics (CFRPs), the intrinsic conductivity of carbon fibers enables piezoresistivity, while in insulating composites like glass fiber-reinforced plastics (GFRPs), conductive nanofillers can be incorporated during polymerization. Carbon-based nanomaterials, have revolutionized nanocomposites research due to their exceptional conductivity, driving significant advancements in this field(Al-Sabagh et al., 2016, 2017).

Electrical conductivity techniques have been widely investigated for detecting failures in carbon fiber-reinforced polymers (CFRPs). Schulte and Baron(Schulte & Baron, 1989) were pioneers in utilizing the intrinsic electrical conductivity of carbon fibers to monitor damage, particularly fiber breakage. Since then, both AC and DC electrical methods have been employed to study damage mechanisms like delamination and matrix cracking under both static and dynamic loading conditions (Abry et al., 2001; Kupke et al., 2001). Flandin and colleagues(Flandin, Brechet, et al., 1999; Flandin, Cavaille, et al., 1999) were among the first to explore nanoscopic conductive fillers with varying aspect ratios in thermoplastic matrices to track macroscopic mechanical strain and damage progression during loading.

In addition, nanoscale and microscale carbon-based materials have been used to modify the matrix of glass-fiber-reinforced thermosetting composites. These studies demonstrated that external stress and mechanical damage in these multiphase composites could be detected via changes in electrical conductivity (Al-Sabagh et al., 2017; Böger et al., 2008a). With advancements in nanotechnology and the growing availability of carbon nanotubes (CNTs) and carbon nanofibers (CNFs), these materials have emerged as promising nanofillers for thermosetting matrix systems. Their exceptional electrical properties, high aspect ratios, and ability to form percolated networks within a viscous matrix make them particularly suited for improving conductivity in these systems. Furthermore, monitoring conductivity changes in the matrix offers significant advantages for damage detection compared to conventional structural health monitoring (SHM) sensors.

This study explores the potential of carbon nanofillers, specifically multi-walled carbon nanotubes (MWCNTs) and carbon nanofibers (CNFs), in enhancing the damage-sensing capabilities of glass fiber-reinforced epoxy (GFRP) composites. The integration of nanofillers in polymer composites has garnered attention due to their ability to improve both mechanical performance and real-time monitoring capabilities, which are critical for structural health monitoring in various industries. By investigating these nanocomposites, we aim to contribute to the development of smart materials that can offer improved durability and reliability in demanding applications.

Experimental:

Materials and Methods:

Materials:

The nanocomposites were prepared using the EPOTUF® 37-127 epoxy system, obtained from U.S. Composites, Inc. (West Palm Beach, FL, USA), with a resin-to-hardener ratio of 2:1. Multi-walled carbon nanotubes (MWCNTs) were supplied by Cheap Tubes®, Inc. (Cambridgeport, VT, USA), and carbon nanofibers (CNFs) were procured from Nanostructured & Amorphous Materials Inc. (Los

Alamos, NM, USA). The reinforcement used was 4.2 oz/yd² bidirectional E-glass fibers, provided by ACP Composites, Inc. (Livermore, CA, USA).

1. Fabrication of GFRP Incorporating Epoxy/Carbon Nanocomposites:

To fabricate the nanocomposite mixtures, 2.0 wt.% of MWCNTs and 2.0 wt.% of CNFs were separately added to the epoxy resin. These mixtures were sonicated at 40°C and 40 kHz for 1 hour. After sonication, the dispersions were subjected to high-shear mixing at 90°C and 11,000 rpm for 1 hour to break up agglomerates, followed by an additional 2 hours of mechanical stirring at 90°C and 800 rpm to further enhance homogeneity. The prepared mixtures were degassed at 50°C for 30 minutes to remove air bubbles and then allowed to cool to room temperature. Subsequently, the hardener was manually mixed into the epoxy resin for 5 minutes.

The prepared epoxy nanocomposites containing 2.0 wt.% CNFs and 2.0 wt.% MWCNTs were used to fabricate glass fiber-reinforced polymer (GFRP) composites. According to ASTM D5687-95, GFRP plates were fabricated using the nanocomposite systems. Six layers of bidirectional glass fiber fabric were laid up with fibers aligned at 0°, and the carbon/epoxy nanocomposite was applied between and over each layer using a roller. Vacuum pressure (3.06 Pa) was applied for 24 hours following the vacuum-assisted wet layup method(Strong, 2008). The GFRP plates were then cured at 100°C for 60 hours to ensure complete polymerization.

Fiber volume fractions for the neat GFRP, 2 wt.% MWCNTs/GFRP, and 2 wt.% CNFs/GFRP composites were measured per ASTM D3171, yielding values of 54.5%, 55.0%, and 55.6%, respectively.

Characterizations:

The cyclic tensile properties of the GFRP composites were evaluated following ASTM D3479-12 using an MTS® Bionix Servo hydraulic system, with data collected by the FlexStar MTS® 793 data acquisition system. Five samples from each GFRP group were tested under load control until failure to assess the fatigue life at a consistent mean stress level. To track damage progression during cyclic loading, a mechanical damage matrix, $D_N(N)$, was computed as a reduction in the secant modulus of elasticity using Equation (1) (Lemaitre & Desmorat, 2005):

$$\boldsymbol{D_N(N) = 1 - \frac{E(N)}{E(0)}} \ \% \tag{1}$$

Where E(0) is the initial modulus of elasticity at the first load cycle, and E(N) is the modulus of elasticity at cycle N.

Electromechanical measurements were also conducted to evaluate the potential of carbon nanoparticles for damage monitoring in GFRP composites. Electrical resistance was measured during the cyclic tension tests using a Keithley 2636B source meter. Conductive electrodes were applied at two points 50 mm apart on the GFRP samples, using silver paint to facilitate the measurements. Additionally, the evolution of damage was quantified by monitoring the changes in electrical conductivity. Figure 1 provides a schematic of the electrical resistance measurement setup used during the static and fatigue tests. Electrical conductivity was monitored, and the electrical damage, $D_E(t)$, was calculated based on changes in conductivity using Equation (2)(Al-Sabagh et al., 2017):

$$\boldsymbol{D_E(t) = 1 - \frac{\sigma(t)}{\sigma(t_0)}} \ \% \tag{2}$$

Where $D_E(t)$ represents electrical damage at time t, $\sigma(t_0)$ is the initial electrical conductivity before loading at time t_0, and $\sigma(t)$ is the electrical conductivity at time t.

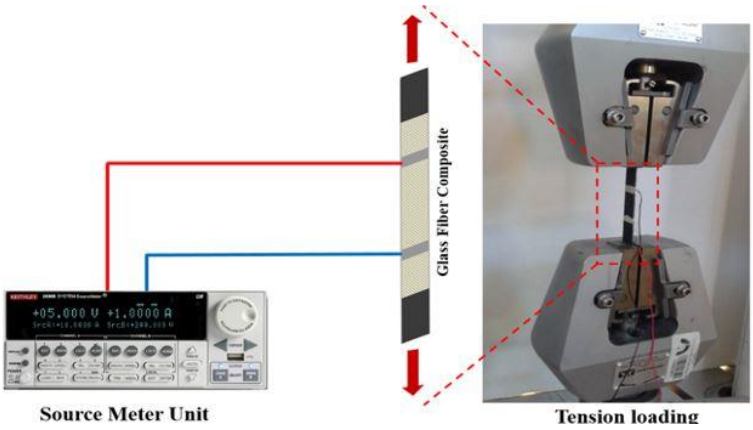

Figure 1: Diagram of electrical resistance measurement of GFRP during fatigue tests.

Results and Discussion

Dynamic Cyclic Tension Test

Figure 2 shows damage propagation in GFRP samples subjected to cyclic stresses. The mechanical damage (D_N) is plotted versus a number of stress cycles observed for Neat/GFRP, CNFs/GFRP and MWCNTs/GFRP samples. It can be observed that the mechanical damage in all GFRP samples decreases gradually during the fatigue cycles until failure. The decrease in the mechanical damage indicates that the GFRP is getting stiffer rather than softer (damaging). The stiffening of the GFRP is actually attributed to the stiffening of the polymer nanocomposite matrix, as the GFRP was loaded off-axis where the matrix rather than the fibers dominate the response(Soliman et al., 2014). This stiffening of the polymer nanocomposite matrix incorporating carbon nanotube under cyclic loading was reported by others and is known as dynamic strain hardening(Carey et al., 2011) . Such behavior was explained by the fact that the morphology of the polymer evolves and gets ordered under repeated elastic stresses in the presence of a carbon nanotube.

Moreover, alternative explanations for such a stiffening phenomenon have been presented. For instance, it was reported that such a response could be attributed to nonlinear stretching and finite extensibility of the network strands (molecular chains between the association links) connecting neighboring network junctions (Creton et al., 2009)(Serero et al., 2000). Another explanation was reported that once a polymer is stressed to a critical value at which it overcomes the intermolecular resistance, the chains begin to orient themselves and induce an orientational hardening (Richeton et al., 2007)(Richeton et al., 2006). Here, since the GFRP sample were tested between 70% and 90% of its tensile strength, such high applied stress caused the networks to rearrange their configuration and stretching of the intermediate chains before the network breaks, resulting in the observed decrease in mechanical damage, indicating an increasing in material stiffness.

Figure 2 also shows a dramatic decrease in the mechanical damage in GFRP-incorporated CNFs and MWCNTs compared with Neat/GFRP. The reason for such behaviour might be attributed to the re-orientation of CNFs and MWCNTs along the loading direction, causing such a significant increase in the composite stiffness. Several works (Petermann & Schulte, 2002) (Berges et al., 2016) reported that when FRP composite incorporated nanofiber subjected to cyclic loading, the fibers tend to straighten and rearrange themselves in the loading direction. Moreover, the pioneering work (Vadlamani et al., 2012) shows the straightening of the uncoiled epoxy matrix incorporated MWCNTs under tensile elongation and MWCNTs tend to partially orient themselves and get close to each other. This self-straightening effect of carbon nanoparticles, as well as the orientational hardening of polymer chains,

caused the observed dramatic increase in the stiffness of the GFRP-incorporated CNFs and MWCNTs compared with Neat/GFRP.

The fatigue life, or number of cycles to failure, for the Neat/GFRP, CNFs/GFRP, and MWCNTs/GFRP samples are displayed in Table 1. The average fatigue life of GFRP was found to be significantly increased when CNFs and MWCNTs were added to the composite, going from $1.04 \pm 0.28)\times10^3$ for Neat/GFRP to $2.77 \pm 0.97\times10^3$ for CNFs/GFRP and to $3.32 \pm 1.32\times10^3$ for MWCNTs/GFRP, which is a 165% and 218% increase, respectively. These nanocomposites have the potential to substantially improve the longevity and durability of GFRP materials, as indicated by the considerable increase in mean fatigue life. Individual GFRP composite samples' fatigue lifes are also displayed in Table 1. Several additional researchers have noted substantial variation in the fatigue life of glass fiber reinforced plastic (GFRP) composites. This variation is thought to be caused by the composites' complicated failure modes, increased sensitivity to batch variability, and overall heterogeneous character(Tomblin & Seneviratne, 2011)(Genedy et al., 2015). The fatigue life for CNFs/GFRP and MWCNTs/GFRP samples is significantly longer than the fatigue life for Neat/GFRP samples, according to statistical analysis using the student t-test with a 95% level of confidence. Statistical analysis did not reveal a significant difference in fatigue life between the CNFs/GFRP and MWCNTs/GFRP samples.

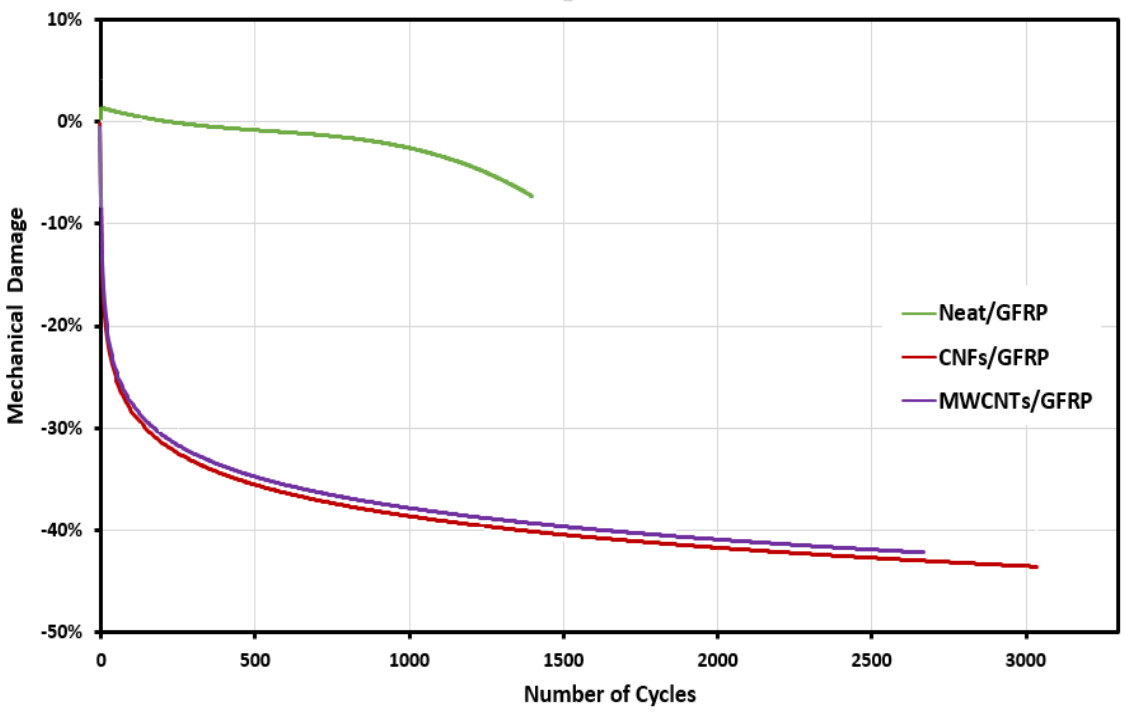

Figure 2: Typical number of cycles vs. mechanical damage (D_N) of all GFRP samples.

Table 1. Fatigue life (Number of cycles until failure) for individual GFRP samples.

Specimens' numbers	Fatigue life		
	Neat/GFRP	CNFs/GFRP	MWCNTs/GFRP
1	1397	3035	2669
2	884	3100	3200
3	1299	4100	4190
4	750	1718	1590
5	900	1908	5000
Mean	1046	2772	3329
Standard deviation	284	974	1323
Percentage deviation	27%	35%	39.7%

Sensing damage propagation in GFRP during cyclic loading:

To investigate damage evolution in GFRP composite samples during cyclic loading, a comparison between the damage metric observed using electrical conductivity monitoring, which was quantified using Equation (2) and that quantified from the cyclic test using Equation (1), was examined. Figures 3 and 4 show damage propagation in GFRP composite samples incorporating CNFs and MWCNTs under cyclic tension, respectively. The mechanical damage (D_N) is plotted versus a number of stress cycles, and the electrical damage (D_E) versus the number of stress cycles for GFRP samples.

It is apparent that as the number of fatigue cycles increased, the electrical damage metric (D_E) increased nonlinearly for both MWCNTs/GFRP and CNFs/GFRP samples, which enables monitoring damage initiation and propagation. Moreover, the electrical damage metrics can be divided into three stages. The first stage until cycle number 100, where a sharp drop in mechanical damage metric takes place. The electrical damage metric of the MWCNTs/GFRP sample decreases due to the straightening of the coiled epoxy chains and their influence on inter-distance between MWCNTs. On the contrary, the electrical damage metric of the CNFs/GFRP sample increases linearly within this stage. The high aspect ratio of MWCNTs compared to that of CNFs played an important role in increasing the possibility of electron hopping and improving electrical conductivity when the MWCNTs get close to each other during the re-orientation of epoxy chains. The second stage is from cycle 100 to 2100 and to 2500 for MWCNTs/GFRP and CNFs/GFRP samples, respectively. A significant increase in the electrical damage metrics takes place within this stage, representing a significant decrease in electrical conductivity due to a decrease in electron hopping density through the matrix barrier owing to the increase of the inter-distance between MWCNTs and between CNFs. The third stage, from cycle 2100 and 2500 to failure for MWCNTs/GFRP and CNFs/GFRP samples, respectively. A very little change in the slope of the electrical damage metric of the MWCNTs/GFRP sample takes place, while in the CNFs/GFRP sample, the electrical damage metric shows an abrupt change in curvature shape. This abrupt change near failure is owing to a faster change in the electrical conductivity due to the initiation and propagation of microcracks in the polymer matrix indicating the failure region.

During overall cycles, the proposed electrical damage metric for the MWCNTs/ GFRP sample showed limited nonlinear sensitivity to damage accumulation during cyclic loading compared with the electrical damage metric for the CNFs/ GFRP sample. The electrical damage metrics increased from zero to 25% in the case of MWCNTs/CFRP and up to 100% in the case of CNFs/GFRP in addition to the unique response of CNFs/GFRP at the failure region, which provides accurate real-time sensing for damage occurring in the CNFs/GFRP composites. It is evident from the above experimental investigation that the damage in GFRP composite can be monitored with high efficiency using the CNFs rather than MWCNTs.

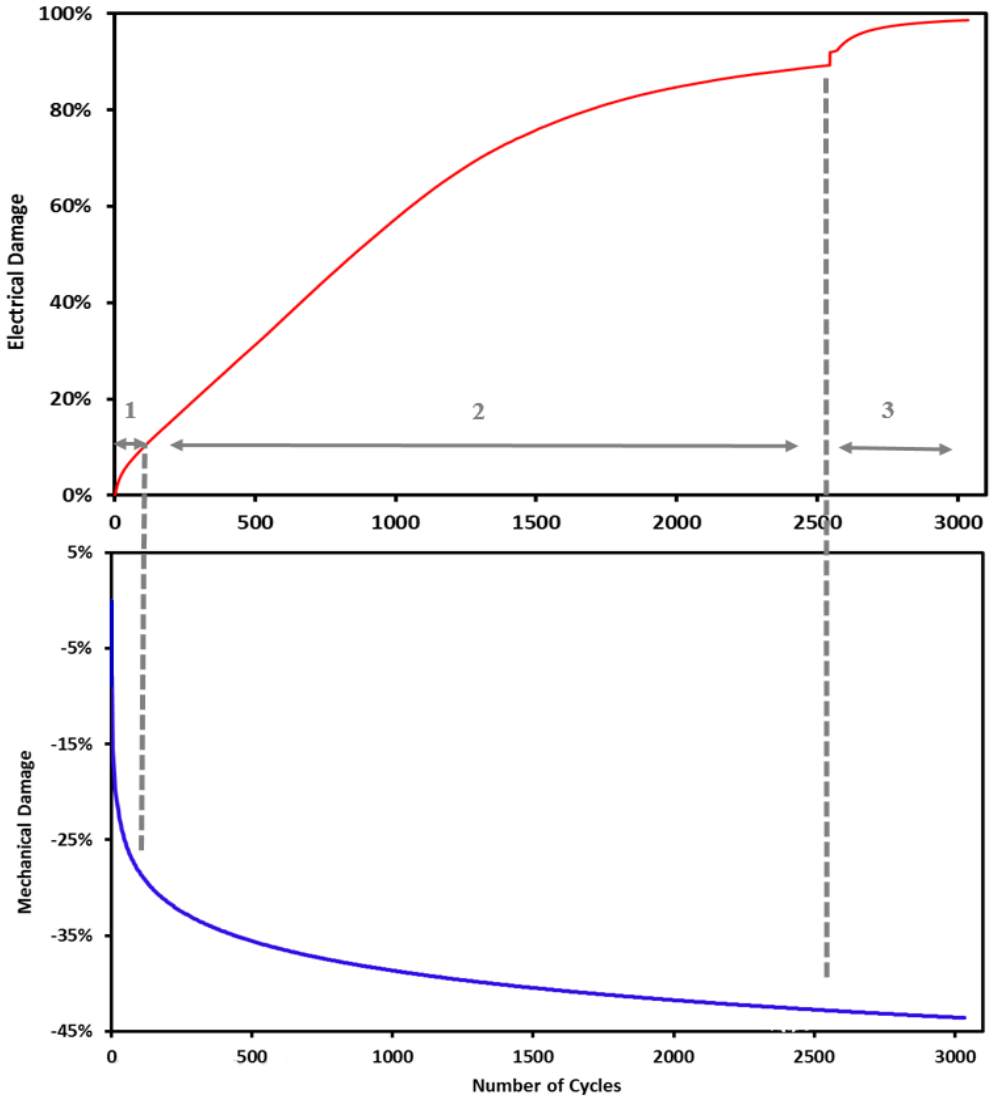

Figure 3: No. of cycles vs. electrical damage (D_E) and no. of cycles vs. mechanical damage (D_N) for glass fiber composite incorporating CNFs under cyclic tension stress.

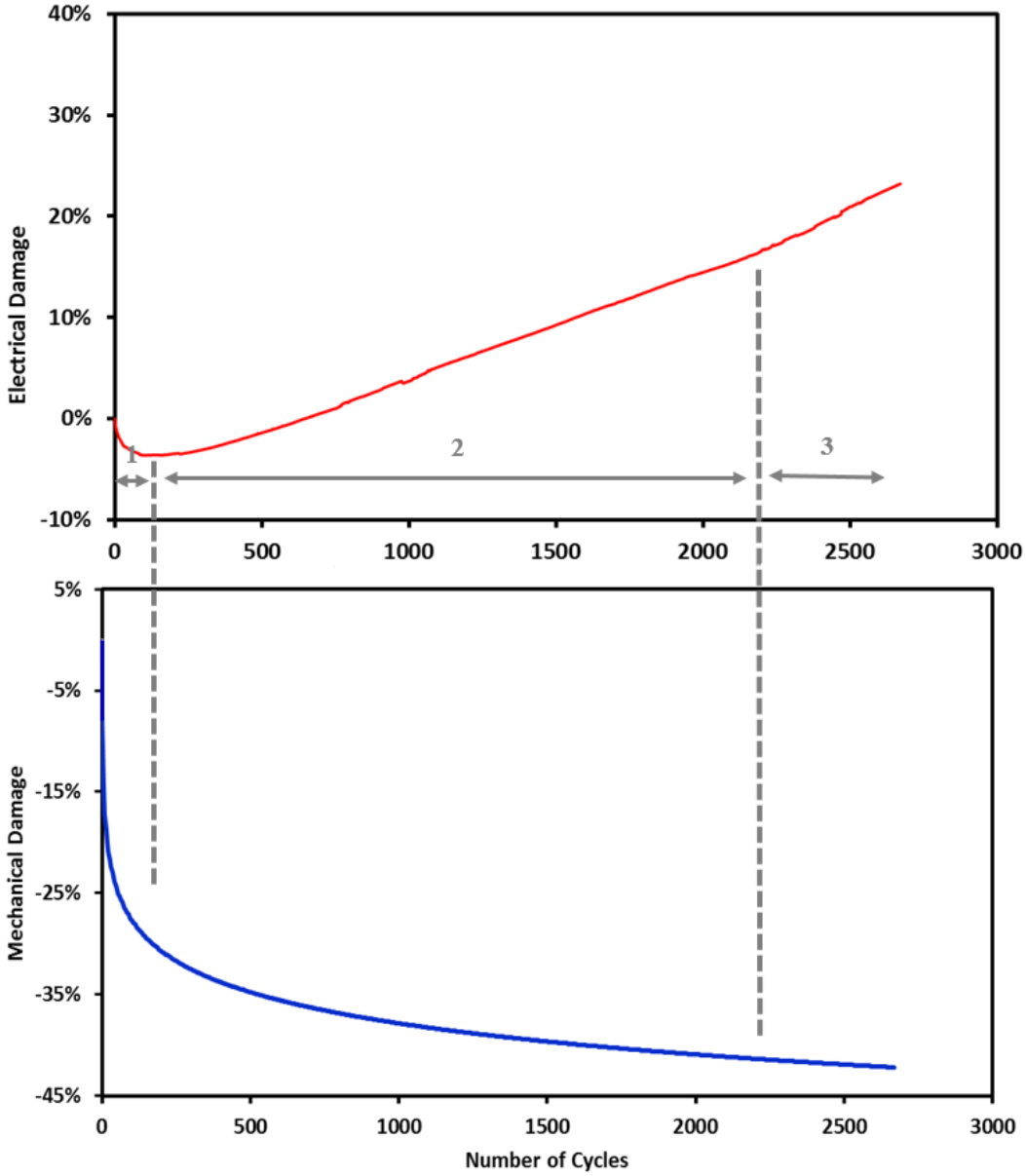

Figure 4: No. of cycles vs. electrical damage (D_E) and no. of cycles vs. mechanical damage (D_N) for glass fiber composite incorporating MWCNTs under cyclic tension stress.

Ultimately, we conclude that the findings of this study align with and expand upon existing research in the field of structural health monitoring (SHM) and damage-sensing capabilities of glass fiber-reinforced composites. The integration of carbon nanofillers, such as carbon nanotubes (CNTs) and carbon nanofibers (CNFs), has been proven to enhance both the mechanical properties and real-time damage detection capabilities of composite materials. To further contextualize our findings, we compare them with existing literature. For instance, studies by Böger et al. demonstrated that incorporating CNTs into GFRP composites significantly improves fatigue performance and enables efficient damage detection through electrical conductivity monitoring (Böger et al., 2008b). Similarly, Keskin and Turan observed electrical resistance changes in GFRP composites during fatigue loading, which is consistent with our findings of electrical conductivity changes tracking damage propagation

(Keskin & Turan, 2024). However, this research goes further by providing a comparative analysis of the performance of CNFs and MWCNTs, showing that CNFs exhibit superior sensitivity in detecting microcracks, which contributes new insights to the field.

Future research will focus on optimizing the dispersion and content of carbon nanofillers to further enhance the damage-sensing capabilities of GFRP composites. Additionally, we plan to explore other types of nanomaterials and hybrid composites to improve the sensitivity of structural health monitoring systems. Scaling up the application of these materials in industries such as aerospace and civil engineering will also be a key focus to validate their practical effectiveness in real-world conditions.

Conclusion

This study demonstrates the potential of carbon nanofillers, specifically multi-walled carbon nanotubes (MWCNTs) and carbon nanofibers (CNFs), in enhancing the damage-sensing capabilities of glass fiber-reinforced epoxy composites. Through combined mechanical and electrical testing, it was shown that these nanocomposite systems exhibit significant potential for monitoring damage under dynamic loading conditions. The incorporation of carbon nanofillers increased the stiffness and fatigue life of the GFRP composites, with CNFs and MWCNTs showing improvements of 165% and 218% in fatigue life, respectively, compared to neat GFRP. Furthermore, the study highlights the effectiveness of electrical conductivity as a real-time damage metric, particularly in composites reinforced with CNFs, offering a promising route for the development of advanced structural health monitoring systems. These findings contribute to the ongoing research on smart composite materials and their applications in industries where reliability and longevity of materials are critical. To inform policy, it is recommended to promote the use of advanced materials with self-monitoring capabilities to enhance safety, reduce maintenance costs, and extend service life across industries. Standardizing technologies for reliable monitoring is also essential.

References

Abry, J. C., Choi, Y. K., Chateauminois, A., Dalloz, B., Giraud, G., & Salvia, M. (2001). In-situ monitoring of damage in CFRP laminates by means of AC and DC measurements. *Composites Science and Technology*, *61*(6), 855–864.

Al-Sabagh, A., Taha, E., Kandil, U., Awadallah, A., Nasr, G. -a. M., & Taha, M. R. (2017). Monitoring moisture damage propagation in GFRP composites using carbon nanoparticles. *Polymers*, *9*(3). https://doi.org/10.3390/polym9030094

Al-Sabagh, A., Taha, E., Kandil, U., Nasr, G.-A., & Taha, M. R. (2016). Monitoring damage propagation in glass fiber composites using carbon nanofibers. *Nanomaterials*, *6*(9). https://doi.org/10.3390/nano6090169

Anas, M., Nasir, M. A., Asfar, Z., Nauman, S., Akalin, M., & Ahmad, F. (2018). Structural health monitoring of GFRP laminates using graphene-based smart strain gauges. *Journal of the Brazilian Society of Mechanical Sciences and Engineering*, *40*(8). https://doi.org/10.1007/s40430-018-1320-4

Berges, M., Léger, R., Placet, V., Person, V., Corn, S., Gabrion, X., Rousseau, J., Ramasso, E., Ienny, P., & Fontaine, S. (2016). Influence of moisture uptake on the static, cyclic and dynamic behaviour of unidirectional flax fibre-reinforced epoxy laminates. *Composites Part A: Applied Science and Manufacturing*, *88*, 165–177.

Böger, L., Wichmann, M. H. G., Meyer, L. O., & Schulte, K. (2008a). Load and health monitoring in glass fibre reinforced composites with an electrically conductive nanocomposite epoxy matrix. *Composites Science and Technology*, *68*(7–8), 1886–1894. https://doi.org/10.1016/j.compscitech.2008.01.001

Böger, L., Wichmann, M. H. G., Meyer, L. O., & Schulte, K. (2008b). Load and health monitoring in glass fibre reinforced composites with an electrically conductive nanocomposite epoxy matrix. *Composites Science and Technology*, *68*(7–8), 1886–1894. https://doi.org/10.1016/j.compscitech.2008.01.001

Carey, B. J., Patra, P. K., Ci, L., Silva, G. G., & Ajayan, P. M. (2011). Observation of dynamic strain hardening in polymer nanocomposites. *ACS Nano*, *5*(4), 2715–2722.

Creton, C., Hu, G., Deplace, F., Morgret, L., & Shull, K. R. (2009). Large-strain mechanical behavior of model block copolymer adhesives. *Macromolecules*, *42*(20), 7605–7615.

Dong, B., Liu, Y., Qin, L., Wang, Y., Fang, Y., Xing, F., & Chen, X. (2016). In-situ structural health monitoring of a reinforced concrete frame embedded with cement-based piezoelectric smart composites. *Research in Nondestructive Evaluation*, *27*(4), 216–229.

Finlayson, R. D., Friesel, M., Carlos, M., Cole, P., & Lenain, J. C. (2001). Health monitoring of aerospace structures with acoustic emission and acousto-ultrasonics. *Insight*.

Flandin, L., Brechet, Y., Canova, G. R., & Cavaillé, J. Y. (1999). AC electrical properties as a sensor of the microstructural evolution in nanocomposite materials: experiment and simulation. *Modelling and Simulation in Materials Science and Engineering*, *7*(5), 865.

Flandin, L., Cavaille, J.-Y., Brechet, Y., & Dendievel, R. (1999). Characterization of the damage in nanocomposite materials by ac electrical properties: experiment and simulation. *Journal of Materials Science*, *34*, 1753–1759.

GangaRao, H. (2017). Infrastructure applications of fiber-reinforced polymer composites. In *Applied Plastics Engineering Handbook* (pp. 675–695). Elsevier.

Genedy, M., Daghash, S., Soliman, E., & Taha, M. M. R. (2015). Improving fatigue performance of GFRP composite using carbon nanotubes. *Fibers*, *3*(1), 13–29.

Güemes, A., Fernandez-Lopez, A., Pozo, A. R., & Sierra-Pérez, J. (2020). Structural health monitoring for advanced composite structures: a review. *Journal of Composites Science*, *4*(1), 13.

Keskin, O., & Turan, F. (2024). Non-destructive health monitoring of glass fibre epoxy composites under fatigue loading using electrical resistance change method. *Nondestructive Testing and Evaluation*. https://doi.org/10.1080/10589759.2024.2395366

Kupke, M., Schulte, K., & Schüler, R. (2001). Non-destructive testing of FRP by dc and ac electrical methods. *Composites Science and Technology*, *61*(6), 837–847.

Lemaitre, J., & Desmorat, R. (2005). *Engineering damage mechanics: ductile, creep, fatigue and brittle failures*. Springer Science & Business Media.

Liang, R., & GangaRao, H. V. (2004). Applications of fiber reinforced polymer composites. *Polymer Composites III 2004*, 173–187.

Li, H. C. H., Herszberg, I., Davis, C. E., Mouritz, A. P., & Galea, S. C. (2006). Health monitoring of marine composite structural joints using fibre optic sensors. *Composite Structures*, *75*(1–4), 321–327.

Petermann, J., & Schulte, K. (2002). The effects of creep and fatigue stress ratio on the long-term behaviour of angle-ply CFRP. *Composite Structures*, *57*(1), 205–210.

Richeton, J., Ahzi, S., Vecchio, K. S., Jiang, F. C., & Adharapurapu, R. R. (2006). Influence of temperature and strain rate on the mechanical behavior of three amorphous polymers: characterization and modeling of the compressive yield stress. *International Journal of Solids and Structures*, *43*(7), 2318–2335.

Richeton, J., Ahzi, S., Vecchio, K. S., Jiang, F. C., & Makradi, A. (2007). Modeling and validation of the large deformation inelastic response of amorphous polymers over a wide range of temperatures and strain rates. *International Journal of Solids and Structures*, *44*(24), 7938–7954.

Schulte, K. and, & Baron, C. (1989). Load and failure analyses of CFRP laminates by means of electrical resistivity measurements. *Composites Science and Technology*, *36*(1), 63–76.

Serero, Y., Jacobsen, V., Berret, J.-F., & May, R. (2000). Evidence of nonlinear chain stretching in the rheology of transient networks. *Macromolecules*, *33*(5), 1841–1847.

Soliman, E., Kandil, U., & Taha, M. R. (2014). Improved strength and toughness of carbon woven fabric composites with functionalized MWCNTs. *Materials*, *7*(6), 4640–4657.

Strong, A. B. (2008). *Fundamentals of composites manufacturing: materials, methods and applications*. Society of Manufacturing Engineers.

Tomblin, J., & Seneviratne, W. (2011). Determining the fatigue life of composite aircraft structures using life and load-enhancement factors. *Final Report, Air Traffic Organization, Washington DC, USA*.

Vadlamani, V. K., Chalivendra, V., Shukla, A., & Yang, S. (2012). In situ sensing of non-linear deformation and damage in epoxy particulate composites. *Smart Materials and Structures*, *21*(7), 75011.

Wang, M. L., Lynch, J. P., & Sohn, H. (2014). Introduction to sensing for structural performance assessment and health monitoring. In *Sensor Technologies for Civil Infrastructures* (pp. 1–22). Elsevier.